

# Transmembrane domain IV of the *Gallus gallus* VT<sub>2</sub> vasotocin receptor is essential for forming a heterodimer with the corticotrophin releasing hormone receptor

**Marina V. Mikhailova**

**Jonathan Blansett**

**Sandie Jacobi**

University of Arkansas for Medical Sciences  
Department of Physiology and Biophysics  
4301 West Markham Street  
Little Rock, Arkansas 72205

**Philip R. Mayeux**

University of Arkansas for Medical Sciences  
Department of Pharmacology and Toxicology  
4301 West Markham Street  
Little Rock, Arkansas 72205

**Lawrence E. Cornett**

University of Arkansas for Medical Sciences  
Department of Physiology and Biophysics  
4301 West Markham Street  
Little Rock, Arkansas 72205

**Abstract.** Corticotrophin releasing hormone receptor (CRHR) and the VT<sub>2</sub> arginine vasotocin receptor (VT2R) are vital links in the hypothalamic-pituitary-adrenal axis that enable a biological response to stressful stimuli in avian species. CRHR and VT2R are both G-protein coupled receptors (GPCRs), and have been shown by us to form a heterodimer via fluorescent resonance energy transfer (FRET) analysis in the presence of their respective ligands, corticotrophin releasing hormone (CRH) and arginine vasotocin (AVT). The dimerization interface of the heterodimer is unknown, but computational analyses predict transmembrane domains (TMs) as likely sites of the interaction. We constructed chimerical VT2Rs, tagged at the C-terminal ends with either cyan fluorescent protein (CFP) or yellow fluorescent protein (YFP), by replacing the fourth transmembrane region (TM4) of VT2R with TM4 of the  $\beta_2$ -adrenergic receptor ( $\beta_2$ AR). The VT2R/ $\beta_2$ AR chimeras were expressed in HeLa cells and proper trafficking is confirmed by observing cell membrane localization using confocal microscopy. VT2R/ $\beta_2$ AR-YFP chimera functionality was confirmed with a Fura-2 acetoxymethyl ester (Fura-2AM) assay. FRET analysis was then performed on VT2/ $\beta_2$ AR-chimera/CRHR pairs, and the calculated distance was observed to be >10 nm apart, indicating that heterodimerization was partly disrupted by mutating TM4 of the VT2R. Therefore, TM4 may form one region of the possible dimerization interfaces between the VT2R and CRHR. © 2008 Society of Photo-Optical Instrumentation Engineers. [DOI: 10.1117/1.2943285]

**Keywords:** hypothalamic-pituitary-adrenal axis; neurohormones; G-protein coupled receptors; receptor interactions.

Paper 07283SSRR received Aug. 3, 2007; revised manuscript received Apr. 11, 2008; accepted for publication Apr. 15, 2008; published online Jun. 27, 2008.

## 1 Introduction

The ability to respond to environmental stress is critical for survival. In birds, stress induces the release of adrenocorticotrophic hormone (ACTH) from corticotrophs in the anterior pituitary gland.<sup>1</sup> ACTH acts on the adrenal cortex to cause secretion of corticosterone, which affects many physiological processes as a part of the stress response. ACTH release is regulated by the hypothalamic hormones corticotrophin releasing hormone (CRH) and either arginine vasopressin (AVP) in mammals or arginine vasotocin (AVT) in nonmammalian vertebrates. Upon release, these hormones enter the portal circulation through the median eminence of the hypothalamus and bind respective receptors present in the cell membrane of corticotrophs. The ability of either hormone to independently elicit secretion of ACTH varies by species, but generally CRH is a more potent secretagogue. In some species, each hormone alone produces a relatively minor effect

on ACTH release, whereas when administered together, a greater than additive or synergistic effect is observed.<sup>2-6</sup> However, the mechanism underlying the greater than additive or synergistic effect of CRH and AVP/AVT on ACTH release is unknown.

The VT2 vasotocin receptor (VT2R) and CRH receptor (CRHR) belong to the G-protein coupled receptor (GPCR) superfamily. GPCRs display a conserved structural motif that consists of an extracellular N-terminus, an intracellular C-terminus, three extracellular loops, three intracellular loops, and seven transmembrane (TM) spanning domains.<sup>7</sup> This architecture is extremely versatile. GPCR ligands include small organic molecules, amines, proteins, and even photons.<sup>8</sup> Upon activation with an agonist, GPCRs associate with and activate heterotrimeric G-proteins, which initiate second messenger signal cascades by stimulating cyclases, lipases, kinases, or other enzymes. GPCRs play vital roles in many cellular and systemic events that include apoptosis, signal transduction, sensory perception, cardiac and smooth muscle regulation, and immunity.<sup>9</sup> Disruption of GPCR function has diverse

Address all correspondence to Marina Mikhailova, Physiology & Biophysics, University of Arkansas for Medical Sciences, 4301 W. Markham St, Slot 750, Little Rock, AR 72205; Tel: (501)-352-2873; Fax: (501)-296-1469; E-mail: mikhailovamarina@uams.edu

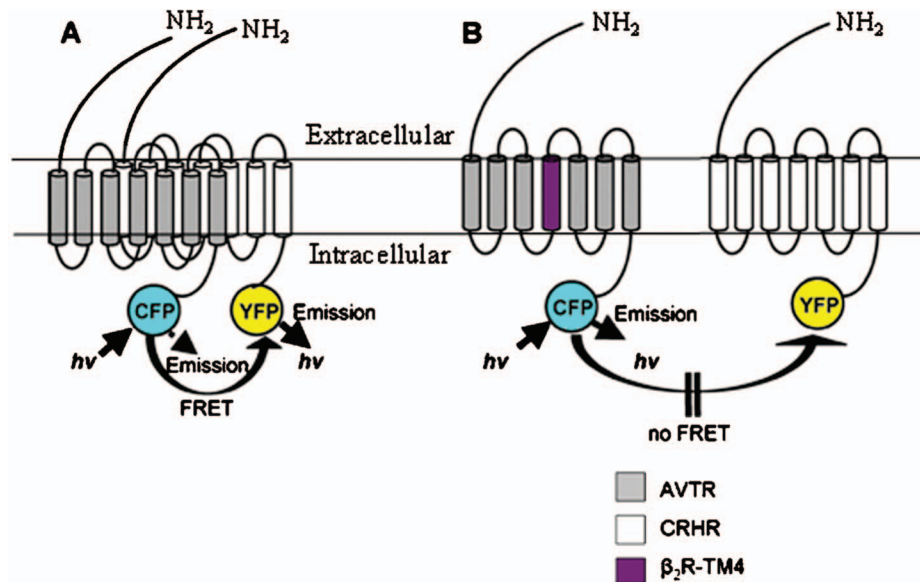


**Fig. 1** Schematic representation of the interaction of the CRHR and VT2R. (a) In the presence of CRH and AVT, FRET measurements indicate that the CRHR and VT2R form heterodimers in which the receptors are  $<10$  nm apart. (b) Repeating the FRET measurement with the CRHR and a chimeric VT2R that substitutes TM4 of the VT2R with TM4 from the  $\beta_2$ AR results in an undetectable FRET signal indicating that the receptors are  $>10$  nm apart.

pathological effects and is the basis of many diseases. Moreover, GPCRs are targets for many pharmacological interventions in the treatment of human diseases. A more thorough knowledge of GPCRs could lead to innovative therapeutics in the future.

Recently, reports of GPCRs forming dimers or higher order oligomers have been published.<sup>10–16</sup> The  $\gamma$ -amino-butyric acid B receptor (GABA<sub>B</sub>R),  $\beta_2$ AR, prostaglandin receptors, and dopamine receptors have all been shown to dimerize at some point in their lifespan. The functional roles of dimerization include proper packaging, transport, and signal transduction.<sup>9</sup> Recent fluorescence resonance energy transfer (FRET) studies have shown that CRHR and VT2 receptors form heterodimers, although the exact residues involved remain unknown.<sup>17</sup> Of the possible dimer interface sites between GPCRs, computational studies have predicted the TMs, specifically TMs 4–6, to be the probable sites of dimerization.<sup>18</sup> By construction of a chimeric VT2R, with TM4 replaced with the TM4 of the  $\beta_2$ AR, and monitoring FRET in the presence of CRH and AVT, we explored the possibility that TM4 of the VT2R participates as one of the possible regions in the formation of the interface of the VT2R-CRHR dimer (Fig. 1).

## 2 Materials and Methods

### 2.1 Preparation of CRHR-YFP/CFP and VT2R-YFP/CFP Constructs

VT2R and CRHR fusion proteins were produced as described previously<sup>17</sup> by cloning either the VT2R or CRHR into pEYFP and pECFP plasmids to obtain a total of four fusion constructs, VT2R-CFP, VT2R-YFP, CRHR-CFP, and CRHR-YFP. Each plasmid was transformed into XL10 Gold *E. coli* cells (Stratagene Inc., La Jolla, CA) and cultured on Luria-Bertani (LB) agar plates with 30  $\mu$ g/ml kanamycin to select

for positive transformants. Single colonies of each fusion were then propagated by inoculating 500 ml LB broth containing 30  $\mu$ g/ml kanamycin and culturing at 37°C with shaking. VT2R and CRHR fusion constructs were purified from *E. coli* cells using a QiaFilter Plasmid Maxi Kit (Qiagen Inc., Valencia, CA) and DNA concentrations were measured spectrophotometrically. Fusion plasmids were screened by *Bam*HI and *Eco*RI (Promega Corp., Madison, WI) restriction endonuclease digestion for proper insertion of AVTR and CRHR DNA sequences.

### 2.2 Site-Directed Mutagenesis

A single point mutation, A206K, in the fluorescent part of the fusion proteins was performed as described previously.<sup>17</sup> Mutations of Ala<sup>206</sup> to Lys in the fluorescent part of pECFP-N1 and pEYFP-N1 expression vectors were made by using the Quick Change site-directed mutagenesis kit (Stratagene), a iCycler Thermal Cycler (BIO-RAD Laboratories, Inc.), and *PfuTurbo* DNA polymerase (Stratagene). The 50  $\mu$ l reaction mixtures each contained approximately 40 ng plasmid template, 125 ng each oligonucleotide primer sense A206K top: 5'-CAG TCC AAG CTG AGC AAA GAC CCC AAC GAG AAG CGC GAT CAC-3' and antisense A206K bottom: 5'-GTG ATC GCG CTT CTC GTT GGG GTC TTT GCT CAG CTT GGA CTG-3'<sup>19</sup> (Integrated DNA Technologies), each deoxynucleoside triphosphate (Stratagene) in a final concentration of 0.05 mM, and 2.5 U *PfuTurbo* DNA polymerase. After a 1-min hot-start at 95°C, 16 cycles of the following program were run: denaturation for 30 sec at 95°C, primer annealing for 1 min at 55°C, and polymerization for 7 min at 68°C. The PCR product was digested for 1 h at 37°C with restriction enzyme *Dpn*I (Stratagene) to eliminate the original template and thereby increase mutation

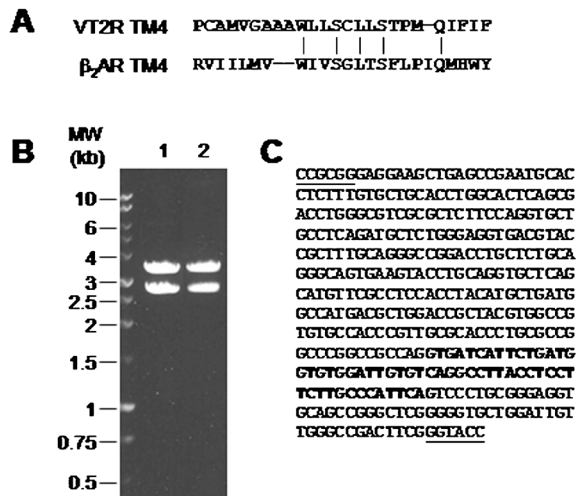


**Fig. 2** Construction of chimeric plasmids. (a) Amino acid alignment of VT2R TM4 and  $\beta_2$ AR TM4 (\* most conservative amino acids) obtained with SIM-alignment tool for protein sequence (<http://www.expasy.ch>): (b) Gel electrophoresis of chimeric VT2R/ $\beta_2$ AR plasmids following digestion with *StuI* to yield expected 3312 bp and 2673 bp fragments. Lane 1: VT2/ $\beta_2$ AR-YFP chimeric plasmid. Lane 2: VT2/ $\beta_2$ AR-CFP chimeric plasmid. (c) Sequence of the  $\beta_2$ AR TM4 domain (bold) with flanking VT2R sequence and the restriction enzyme sites underlined.

efficiency. The DNA sequences of the mutated plasmids were verified by sequencing.

### 2.3 Preparation of VT2R/ $\beta_2$ AR Chimeras

As described in Fig. 2, a 383 bp sequence containing TM4 of the  $\beta_2$ AR, flanked on both 5' and 3' ends with the VT2R sequence to incorporate endogenous *SacII* and *KpnI* restriction sites, was synthesized and cloned into a pUC57 vector (EZ Biolabs, Westfield, IN). The pUC57-VT2R/ $\beta_2$ AR-TM4 vector was digested with *SacII* and *KpnI* restriction enzymes (New England Biolabs, Ipswich, MA) and the digestion product was separated by gel electrophoresis on a 1% TBE agarose gel to obtain the now 380 bp fragment with the  $\beta_2$ AR TM4 insertion, flanked on both sides with VT2R sequence. This 380 bp fragment was gel-purified via a QIAquick Gel Extraction Kit (Qiagen). VT2R-YFP/CFP fusion plasmids were digested with *KpnI* and *SacII* and the digestion products were separated on a 1% agarose gel to obtain the 5985 bp pEYFP/pECFP fragments, which were gel-purified. Complementary gel-purified DNA fragments were then ligated (Fig. 2) with T4 DNA ligase in 2X rapid ligation buffer (Promega), and transformed into XL10 Gold *E. coli*. Cells were grown on agarose plates with 30  $\mu$ g/ml kanamycin. Positive transformants were screened for proper insertion by *StuI* (Invitrogen) digestion and sequenced to further confirm that the  $\beta_2$ AR-TM4 insertion was present in pEYFP/CFP-VT2R plasmids, and to ensure that no mutations had incurred in either the VT2R, CFP, or YFP sequences.

### 2.4 Transfection of HeLa Cells with CRHR-CFP/YFP, VT2R-CFP/YFP Fusion Plasmids, and VT2R/ $\beta_2$ AR-CFP/YFP Chimeras

HeLa cells were cultured in a 95% air/5% CO<sub>2</sub> incubator at 37°C and plated on sterile coverslips in a six-well plate at a density of 40,000–60,000 cells/well in 2 ml Eagle minimal essential media (MEM, ATCC, Manassas, VA) supplemented with 10% fetal bovine serum (FBS). Liposomes were created by diluting 2  $\mu$ g of respective fusion or chimeric receptor DNA with 250  $\mu$ l MEM, and combining with 10  $\mu$ l of Lipofectamine 2000 (Invitrogen) which had been diluted in 250  $\mu$ l MEM, gently shaken, and incubated for 5 min at room temperature. The receptor DNA/Lipofectamine mixture was incubated 20 min at room temperature to allow for liposome formation, after which 500  $\mu$ l was added to the appropriate well to reach a total volume of 2.5 ml. HeLa cells were cultured for 4 h, after which time the media was changed with fresh MEM-10% FBS media. The cells were then cultured additionally for 12 h and visualized with confocal microscopy to localize the receptor.

### 2.5 Visualization of Chimeric Receptors

Cells were visualized by mounting the cover slips from each well of each respective transfection on slides and viewing with a Zeiss LSM 510 Meta confocal microscope (Carl Zeiss, New York, NY). A 514-nm laser was used to excite YFP-tagged receptors, while a 458-nm laser was applied to excite CFP-tagged receptors. Images were adjusted to attain maximal resolution. A digital transformation of images was not applied.

### 2.6 Hormonal Treatment

Treatment of cells with AVT or CRH was performed as described previously.<sup>17</sup> Briefly, AVT and CRH were diluted into modified receptor buffer (10 mM KCl, 10 mM MgCl<sub>2</sub>, 2 mM EGTA, 20 mM Hepes, 120 mM NaCl, 1 mg/ml BSA, pH 7.4) as previously suggested.<sup>20</sup> HeLa cells transiently transfected with CRHR-, VT2R-, and VT2/ $\beta_2$ AR-fusion protein constructs were incubated with 100 nM human CRH and 100 nM (Arg8)-vasotocin for 20 min at 37°C.

### 2.7 Fura-2AM Calcium Mobilization Assay

HeLa cells were cultured in a 95% air/5% CO<sub>2</sub> incubator at 37°C and plated in twelve 10-cm dishes. Four plates were transfected with VT2R-YFP fusion plasmids, four plates were transfected with VT2R/ $\beta_2$ AR-YFP chimeras, and four plates were not transfected and served as a negative control. Liposomes were made by combining 24  $\mu$ g of respective DNA, diluted in 1.5 ml MEM, with 60  $\mu$ l Lipofectamine 2000 in 1.5 ml MEM, gently shaken, and incubated at room temperature for 5 min. Three ml of respective liposomes were then added to the appropriate plates, which contained 12 ml 10% FBS-MEM. Cells were cultured for 40 h at 37°C in a humidified CO<sub>2</sub> incubator. Fresh 10% FBS-MEM was added 4 h posttransfection, and 10% FBS-MEM with 1% penicillin-streptomycin fungizone (Invitrogen) was added 16 h posttransfection. Cells were harvested and washed twice with

10 ml phosphate buffered saline (PBS). Cells were then resuspended in Gey's buffer and the Fura-2AM assay was performed as previously described.<sup>21</sup>

## 2.8 FRET Analysis

As described above, HeLa cells were grown on cover slips placed on the bottom of 6-well plates for 24 h. Prior to transfection with CFP/YFP constructs, the cover slips were moved to new 6-well plates containing fresh media. Twenty-four hours after transfection, the fluorescent fusion proteins were visualized in intact cells. Images were collected by using Carl Zeiss 510 META laser scanning confocal microscope with a 40× water immersion objective. LSM Image Browser Software was used for collection of images. CFP was excited at 457 nm (power 118 μW) and observed from 485/30 nm. YFP was excited at 514 nm (power 29 μW), observed from 545/40 nm. Images from all single-labeled (CFP or YFP fusion proteins samples) or double-labeled (CFP and YFP fusion proteins) specimens were taken under exactly the same conditions (PCM 1024 × 1024 color, 2.3× zoom, without processing). There are two contaminants in the FRET signal: donor cross talk and acceptor bleed through. We used the previously developed algorithm,<sup>22</sup> which removes these contaminants pixel by pixel on the basis of matched fluorescence levels between the double-labeled specimen and a single-labeled reference specimen, using seven images: two single-labeled donor reference images (donor excitation/donor channel and acceptor channel); two single-labeled acceptor reference images (donor and acceptor excitation, both in the acceptor channel); and three double-labeled images (acceptor excitation/acceptor channel, and donor excitation/donor and acceptor channels). This algorithm allowed the capture of a pure FRET image with following E% analysis and distance calculation. With these values, the FRET data were corrected for cross talk and filter leaks as well as potential differences in the concentrations of the donor and acceptor. A background (region with no cells) was subtracted from the foreground value (region within the cell). Approximately five images were taken from each specimen; six to eight regions of interest (ROI) on cell membranes were chosen from each image.

## 3 Results

### 3.1 VT2R/β<sub>2</sub>AR-YFP/CFP Chimera Construction

Proper insertion of the β<sub>2</sub>AR-TM4 sequence into VT2R-YFP and VT2R-CFP fusion proteins was confirmed by *StuI* digestion [Fig. 2(b)] and sequencing [Fig. 2(c)]. The sequencing identified that the TM4 of the chimeric receptors was represented by 19 amino acid from the β<sub>2</sub>-adrenergic receptor. As expected, the rest of the DNA sequences of each construct contained no other mutations.

### 3.2 VT2R/β<sub>2</sub>AR-YFP/CFP Chimera Localization and Functionality

In order to prove that function correlates with correct trafficking, two chimeras, VT2/β<sub>2</sub>AR chimera tagged with the donor or acceptor and CRHR tagged with the acceptor or donor, were prepared. Following transfection of HeLa cells, both fusion proteins were localized mainly in cytoplasmic membrane (Fig. 3). We next determined whether the chimeric receptors

were capable of responding to AVT by mobilizing intracellular Ca<sup>2+</sup> and thus are functionally active. For this, only VT2R-YFP and VT2/β<sub>2</sub>AR-YFP chimeric receptor constructs were used to prevent an overlap with the Fura-2 fluorescence that occurs with the CYP fluorochrome. Using nontransfected HeLa cells as a control, the addition of AVT did not cause any change in Ca<sup>2+</sup> mobilization as measured using Fura-2 [Fig. 4(a)]. In cells expressing either the VT2R or the VT2/β<sub>2</sub>AR chimeric receptor, identical increase of Fura-2 fluorescence was observed indicating that Ca<sup>2+</sup> mobilization was equal between the two expressed proteins [Fig. 4(b) and 4(c)]. These data suggest that the overexpressed chimera receptor was able to activate downstream signal transduction pathways and mobilize intracellular Ca<sup>2+</sup>.

### 3.3 FRET Analysis

It is known that dimers can be formed between two EFP parts regardless of the existence of any other dimerization of the proteins fused to these fluorescent proteins.<sup>19</sup> A single point mutation, A206K, in the fluorescent part of any fusion protein has been shown to prevent the formation of nonspecific dimerization.<sup>19</sup> To demonstrate that a FRET signal results from a specific interaction between the CRHR and VT2R rather than a nonspecific interaction occurring between the fluorophores, the site-directed mutation of Ala<sup>206</sup> to Lys was performed in fluorescent parts of the CRHR-CFP, VT2R-CFP, VT<sub>2</sub>R-YFP fusion proteins, VT2R/β<sub>2</sub>AR-CFP, and VT2R/β<sub>2</sub>AR-YFP. The mutated variants of the fusion proteins were expressed in the same cellular compartments as wild-type receptors (data not shown). All FRET experiments were obtained with mutated A206K variants of fusion proteins.

The ability to form heterodimers between CRHR and VT2 receptor and between CRHR and the chimera VT2/β<sub>2</sub>AR receptor was studied in transfected HeLa cells using FRET analysis. This method detects the transfer of excitation energy from donor fluorophore to a nearby acceptor that can occur only over a distance of about 3–7 nm.<sup>22–24</sup> In order to obtain a quantitative measure of heterodimer formation, image data were processed using PFRET software obtained from the W. K. Keck Center for Cellular Imaging (University of Virginia, Charlottesville, VA, www.kcci.virginia.edu).<sup>22,25</sup> Quantitative FRET analysis as described previously<sup>17</sup> demonstrated that cotransfection of HeLa cells with CRHR-CFP and VT2R-YFP resulted in a constitutive resonance energy transfer between the fluorescence donor and acceptor. Addition of either CRH or AVT alone resulted in a slight, but not a statistically significant, enhancement of FRET efficiency, whereas simultaneous addition of the two hormones resulted in a significant ( $p < 0.001$ ) increase in FRET efficiency (Fig. 5). The FRET efficiency reached 29–36%, and the distance between subunits was 6–7 nm.

Quantitative FRET analysis demonstrated that substitution of TM4 from the VT2R with TM4 from the β<sub>2</sub>AR affects the interaction between the two receptor proteins (Fig. 5). FRET analysis of HeLa cells cotransfected with CRHR-CFP and VT2R/β<sub>2</sub>AR-YFP (Figs. 3 and 5) after separate or simultaneous addition of CRH and AVP hormones demonstrated that the FRET efficiency was 8–12% and the distance increased to 9–12 nm. As with VT2/β<sub>2</sub>AR-CFP and CRHR-YFP recep-

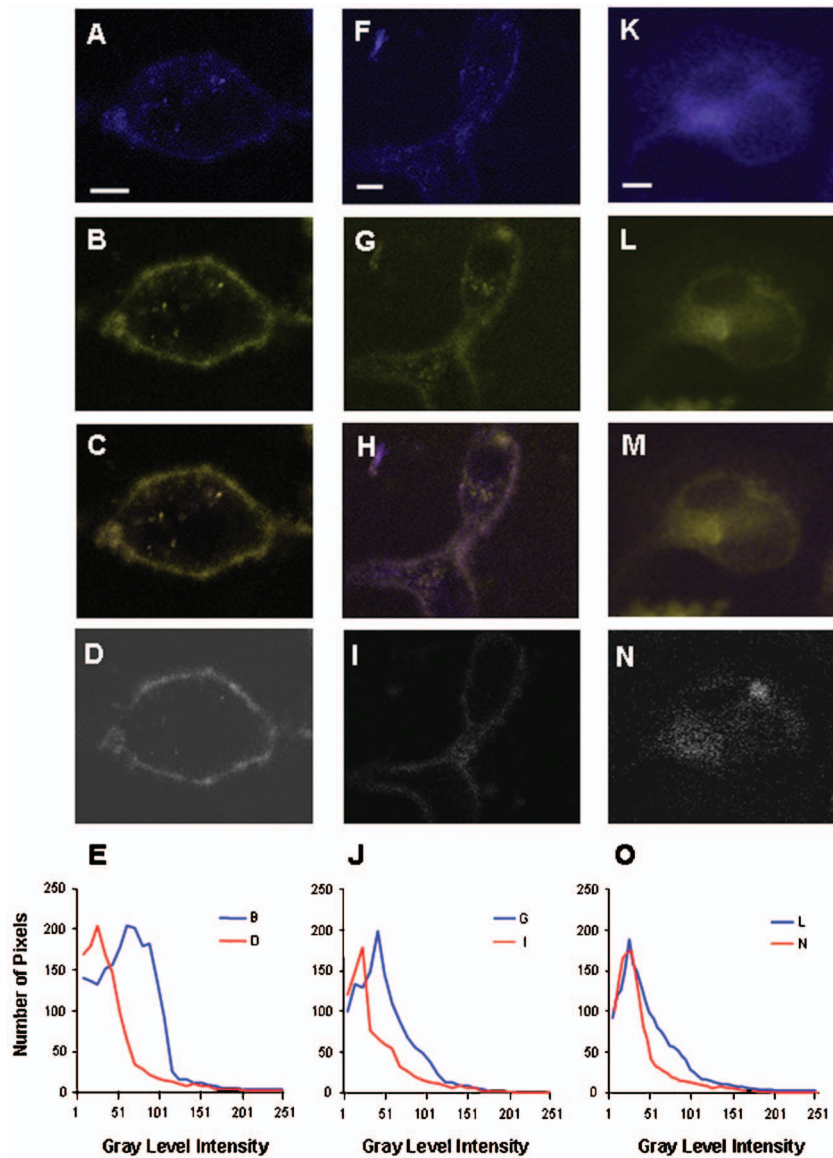


**Fig. 3** Images for algorithm FRET method. Laser scanning confocal images in HeLa cells are shown for CRHR-CFP and VT2R-YFP (a, b, c, d), CRHR-CFP and VT2R/ $\beta_2$ AR-YFP chimeric receptor (f, g, h, i), and CRHR-YFP and VT2R/ $\beta_2$ AR-CFP chimeric receptor (k, l, m, n). The associated histograms are shown for CRHR-CFP and VT2R-YFP (e), CRHR-CFP and VT2R/ $\beta_2$ AR-YFP (j), and CRHR-YFP and VT2R/ $\beta_2$ AR-YFP (o). HeLa cells were labeled with CFP (donor, CRHR or VT2R/ $\beta_2$ AR) and YFP (acceptor, VT2R, VT2R/ $\beta_2$ AR or CRFR). To set the parameters for quantitative FRET, the images of HeLa cells expressing only CRHR-CFP or VT2R/ $\beta_2$ AR-CFP and either VT2R-YFP or VT2R/ $\beta_2$ AR-YFP or CRFR-YFP were taken with donor and acceptor filter sets (images are not shown). Using confocal microscopy, processed FRET (PFRET) fluorescence signals (nonradioactive transfer of energy from CRHR or VT2R/ $\beta_2$ AR donor fluorophore to VT2R or VT2R/ $\beta_2$ AR or CRHR acceptor fluorophore) were collected in the double-labeled cells. Images are representative of five experiments. Images collected during double-labeled donor excitation, donor channel revealing the distribution of CRHR-CFP (a and f) or VT2R/ $\beta_2$ AR-CFP (k); double-labeled, donor excitation, acceptor channel (b, g, and l); double-labeled acceptor excitation, acceptor channel revealing the distribution of VT2R-YFP (c), VT2R/ $\beta_2$ AR-YFP (h), or CRHR-YFP (m). (d, i, and n) PFRET calculated with algorithm methods. Scale bar: 20  $\mu$ M.

tors, FRET efficiency was 9–13% and the distance increased to 10–12 nm.

#### 4 Discussion

Compelling evidence is accumulating in the literature that GPCRs can be organized in the cell membrane as homo- or hetero-oligomers.<sup>10–16</sup> Both computational and experimental efforts have been made to understand the basis of protein-protein interaction in GPCR oligomerization. The GABA<sub>B</sub>R,

$\beta_2$ AR, prostaglandin receptors, and dopamine receptors have all been shown to dimerize at some point in their lifespan. Functional roles of dimerization include proper packaging, transport, and signal transduction, among others,<sup>9</sup> but the specific molecular determinants required for receptor-receptor oligomerization are still unknown.

Recent (FRET) studies have shown that CRHR and AVTR heterodimerize on the cell membrane of living cells, although the exact residues involved remain unknown.<sup>17</sup> Moreover, it

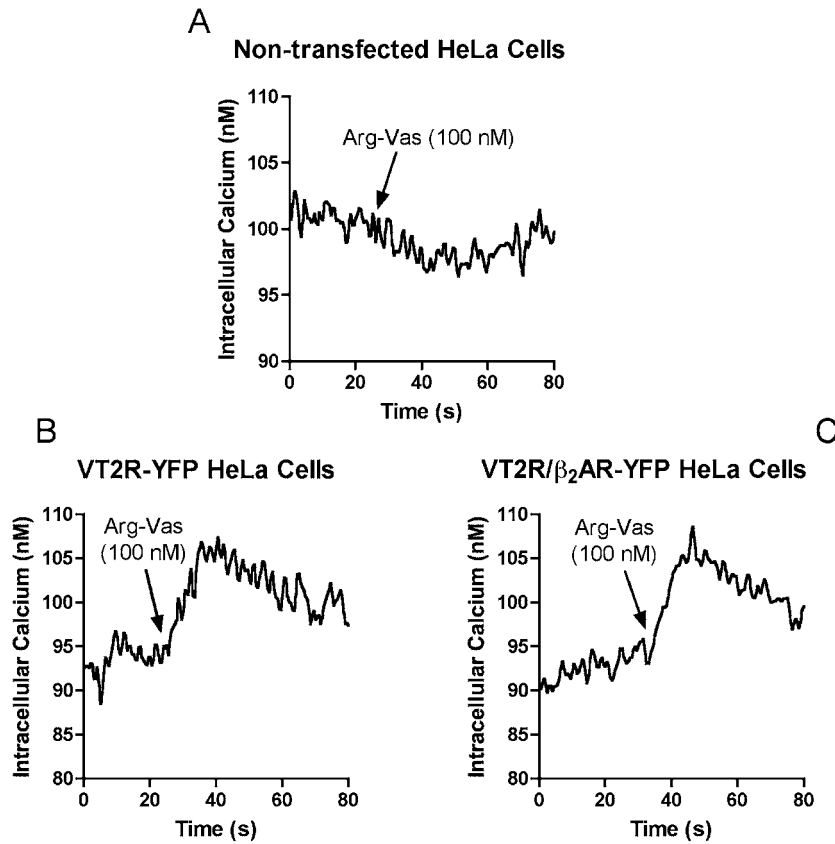


**Fig. 4** Calcium mobilization in HeLa cells expressing either the VT2R or the VT2/β<sub>2</sub>AR chimeric receptor in response to AVT. HeLa cells were either not transfected or transfected with plasmids expressing VT2R-YFP or VT2/β<sub>2</sub>AR-YFP. Cells were subsequently treated with 100 nM AVT and changes in fura-2 fluorescence were used to monitor intracellular Ca<sup>2+</sup> levels. (a) A representative tracing from nontransfected cells demonstrating nonresponsiveness to AVT. (b) Representative tracing from HeLa cells expressing VT2R-YFP demonstrating mobilization of intracellular Ca<sup>2+</sup> upon addition of AVT. (c) Representative tracing from HeLa cells expressing the VT2/β<sub>2</sub>AR chimeric receptor demonstrating mobilization of intracellular Ca<sup>2+</sup> upon addition of AVT.

was demonstrated that human V1bR and CRHR1 can form constitutive homo- and heterodimers.<sup>26</sup> An atomic-force microscopy analysis of native retinal disk membranes has revealed an organization of molecules of the prototypic GPCR rhodopsin in paracrystalline arrays. Based on these data, the fourth and fifth transmembrane helices (TM4 and TM5) have been inferred to be involved in intraic contact, whereas helices TM1 and TM2, and the cytoplasmic loop connecting helices TM5 and TM6, have been inferred to facilitate the formation of rhodopsin dimer rows. It is not clear, however, whether all GPCRs use these same interfaces or whether some GPCRs use different oligomerization interfaces to achieve functional selectivity. Recent computational and experimental data suggest the involvement of different TM regions in forming the dimerization interface of highly related GPCRs. These findings are also consistent with the possible organization of these receptors into higher-order oligomers, with multiple distinct oligomeric interfaces. As it becomes clearer that oligomeric structures are important for activation<sup>27</sup> and have physiological relevance,<sup>28</sup> functional models of GPCR dimers/oligomers are needed to characterize the structural context of receptor association, and its implication in receptor function.

Previous studies from our laboratory using FRET analysis determined that the VT2R and CRHR form specific heterodimers in the presence of both AVT and CRH.<sup>17</sup> The logi-

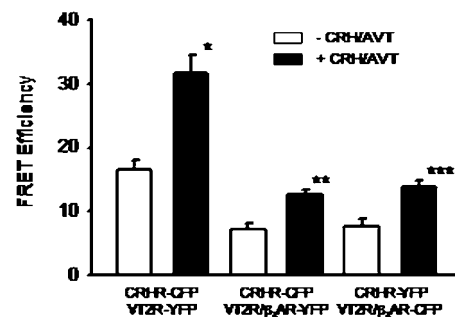


**Fig. 5** FRET efficiency in CRHR and either VT2R or VT2R/β<sub>2</sub>AR-expressing HeLa cells following treatment with CRH and AVT. HeLa cells were either transfected with plasmids expressing CRHR-CFP and VT2R-YFP, CRHR-CFP and VT2/β<sub>2</sub>AR-YFP, or with VT2/β<sub>2</sub>AR-CFP and CRHR-YFP and 24 h later were treated with either vehicle or 100 nM CRH and 100 nM AVT together. FRET measurements were taken 30 min after hormone addition. Data are the means ± SEM (n=5). \*FRET efficiency was significantly different (p < 0.011) than that measured in HeLa cells expressing CRHR-CFP and VT2R that were not treated with the hormones. \*\*FRET efficiency was significantly different (p < 0.008) than that measured in HeLa cells expressing CRHR-CFP and VT2/β<sub>2</sub>AR-YFP that were not treated with the hormones. \*\*\* FRET efficiency was significantly different (p < 0.02) than that measured in HeLa cells expressing CRHR-YFP and VT2/β<sub>2</sub>AR-CFP that were not treated with the hormones.

cal next step to extend this observation would be to find the dimerization interfaces between the two receptors. The three-dimensional architectures of VT2R and CRHR have not been solved, as GPCRs are inherently hard to crystallize due to their relatively insoluble, lipophilic TM regions. Recent computational studies on GPCRs have predicted the TM regions to be likely sites of physical interaction in class A GPCRs.<sup>18</sup> As a member of the class A GPCR family, we elected to alter the TM4 of the AVTR in an attempt to disrupt dimerization with CRHR, a member of the class B GPCR family.

If the substitution of TM4 of the VT2R with TM4 of the  $\beta_2$ AR had compromised either the localization or functionality of the chimerical receptors, very few conclusions could be drawn about the significance of the FRET analysis. The observed membrane localization of the VT2R-YFP and VT2R-CFP chimeras implies that the substitution of TM4 from the  $\beta_2$ AR did not compromise proper packaging, folding, or trafficking of the receptor to the cell membrane. Upon ligand binding, the VT2R couples to and activates G<sub>q</sub>, which activates phospholipase C, which in turn mobilizes Ca<sup>2+</sup> from the endoplasmic reticulum. If the chimeric receptor was not functional, the tertiary structure of the protein may have been altered enough to abolish any functional or pharmacological activity of TM4, such as dimerization with CRHR. The ability of the VT2R/ $\beta_2$ AR-YFP chimera to mobilize Ca<sup>2+</sup> upon exposure to AVT at levels similar to those of the VT2-YFP fusion protein implies that the chimera was not mutated beyond the point of functionality.

In conclusion, a chimeric receptor, VT2R/ $\beta_2$ AR-YFP, was prepared and was found to activate Ca<sup>2+</sup> mobilization upon AVT addition in transfected HeLa cells. Using FRET analysis it was demonstrated that VT2R/ $\beta_2$ AR chimeras and CRHR, as well as VT2R and CRHR, exist in the close proximity to each other in the membrane. The addition of the CRH/AVT ligands increase FRET significantly, two-fold for both wild-type and VT2R/ $\beta_2$ AR chimera (Fig. 5), and confirm dimerization of the receptors, as the response for the ligand addition. FRET efficiency was at a significantly low rate with chimera receptors (15%) compared to that with wild type receptors (36%); the possibility of chimeric receptors to form heterodimers with the CRHR in the presence of CRH and AVT was diminished, but not blocked completely.

Our results suggest that TM4 of VT2R may play a role in the formation of heterodimers between the VT2R and CRHR. However, our results do not exclude the possibility that other VT2R regions, notably other transmembrane domains, are involved in the dimerization between the VT2R and CRHR. Studies are under way to determine the involvement of additional VT2R transmembrane domains in the formation of dimer pairs with the CRHR.

### Acknowledgments

Special thanks to Brian Shank for his assistance with confocal microscopy, as well as the DNA Damage Core Center and the Digital Confocal Microscopy Laboratory at the University of Arkansas for Medical Sciences. This research was supported by NIH P20 RR16460 and NSF IBN0111006.

### References

1. D. A. Baeyens and L. E. Cornett, "The cloned avian neurohypophysial hormone receptors," *Comp. Biochem. Physiol., Part B: Biochem. Mol. Biol.* **143**(1), 12–19 (2006).
2. B. I. Baker, D. J. Bird, and J. C. Buckingham, "In the trout, CRH and AVT synergize to stimulate ACTH release," *Regul. Pept.* **67**(3), 207–210 (1996).
3. Y. Arsenijevic, M. Dubois-Dauphin, E. Tribollet, M. Manning, W. H. Sawyer, and J. J. Dreifuss, "Vasopressin-binding sites in the pig pituitary gland: competition by novel vasopressin antagonists suggests the existence of an unusual receptor subtype in the anterior lobe," *J. Endocrinol.* **141**(3), 383–391 (1994).
4. D. A. Leong, "A complex mechanism of facilitation in pituitary ACTH cells: recent single-cell studies," *J. Exp. Biol.* **139**, 151–168 (1988).
5. A. N. Brooks and J. R. Challis, "Effects of CRF, AVP and opioid peptides on pituitary-adrenal responses in sheep," *Peptides* **10**(6), 1291–1293 (1989).
6. F. A. Antoni, "Vasopressinergic control of pituitary adrenocorticotropin secretion comes of age," *Front Neuroendocrinol* **14**(2), 76–122 (1993).
7. J. Bockaert and J. P. Pin, "Molecular tinkering of G protein-coupled receptors: an evolutionary success," *EMBO J.* **18**(7), 1723–1729 (1999).
8. U. Gether and B. K. Kobilka, "G protein-coupled receptors. II. Mechanism of agonist activation," *J. Biol. Chem.* **273**(29), 17979–17982 (1998).
9. R. Maggio, F. Novi, M. Scarselli, and G. U. Corsini, "The impact of G-protein-coupled receptor hetero-oligomerization on function and pharmacology," *FEBS Lett.* **272**(12), 2939–2946 (2005).
10. S. Terrillon, C. Barberis, and M. Bouvier, "Heterodimerization of V1a and V2 vasopressin receptors determines the interaction with beta-arrestin and their trafficking patterns," *Proc. Natl. Acad. Sci. U.S.A.* **101**(6), 1548–1553 (2004).
11. J. A. Javitch, "The ants go marching two by two: Oligomeric structure of G-protein-coupled receptors," *Mol. Pharmacol.* **66**(5), 1077–1082 (2004).
12. G. Milligan, D. Ramsay, G. Pascal, and J. J. Carrillo, "GPCR dimerization," *Life Sci.* **74**(2–3), 181–188 (2003).
13. M. Matsuda, T. Imaoka, A. J. Vomachka, G. A. Gudelsky, Z. Hou, M. Mistry, J. P. Bailey, K. M. Nieport, D. J. Walther, M. Bader, and N. D. Horseman, "Serotonin regulates mammary gland development via an autocrine-paracrine loop," *Dev. Cell* **6**(2), 193–203 (2004).
14. P. S. Park, S. Filipek, J. W. Wells, and K. Palczewski, "Oligomerization of G protein-coupled receptors: past, present, and future," *Biochemistry* **43**(50), 15643–15656 (2004).
15. M. Filizola and H. Weinstein, "The structure and dynamics of GPCR oligomers: a new focus in models of cell-signaling mechanisms and drug design," *Curr. Opin. Drug Discov. Devel.* **8**(5), 577–584 (2005).
16. D. Fotiadis, B. Jastrzebska, A. Philippson, D. J. Muller, K. Palczewski, and A. Engel, "Structure of the rhodopsin dimer: a working model for G-protein-coupled receptors," *Curr. Opin. Struct. Biol.* **16**(2), 252–259 (2006).
17. M. V. Mikhailova, P. R. Mayeux, A. Jurkevich, W. J. Kuenzel, F. Madison, A. Periasamy, Y. Chen, and L. E. Cornett, "Heterooligomerization between vasotocin and corticotropin-releasing hormone (CRH) receptors augments CRH-stimulated 3',5'-cyclic adenosine monophosphate production," *Mol. Endocrinol.* **21**(9), 2178–2188 (2007).
18. M. Filizola and H. Weinstein, "The study of G-protein coupled receptor oligomerization with computational modeling and bioinformatics," *FEBS Lett.* **272**(12), 2926–2938 (2005).
19. D. A. Zacharias, J. D. Violin, A. C. Newton, and R. Y. Tsien, "Partitioning of lipid-modified monomeric GFPs into membrane microdomains of live cells," *Science* **296**(5569), 913–916 (2002).
20. D. M. Dorsa, L. A. Majumdar, F. M. Petracca, D. G. Baskin, and L. E. Cornett, "Characterization and localization of 3H-arginine-8-vasopressin binding to rat kidney and brain tissue," *Peptides* **4**(5), 699–706 (1983).
21. F. L. Tan, S. J. Lolait, M. J. Brownstein, N. Saito, V. MacLeod, D. A. Baeyens, P. R. Mayeux, S. M. Jones, and L. E. Cornett, "Molecular cloning and functional characterization of a vasotocin receptor subtype that is expressed in the shell gland and brain of the domestic chicken," *Biol. Reprod.* **62**(1), 8–15 (2000).
22. M. Elangovan, H. Wallrabe, Y. Chen, R. N. Day, M. Barroso, and A.

- Periasamy, "Characterization of one- and two-photon excitation fluorescence resonance energy transfer microscopy," *Methods* **29**(1), 58–73 (2003).
23. M. Marcelli, G. R. Cunningham, S. J. Haidacher, S. J. Padayatty, L. Sturgis, C. Kagan, and L. Denner, "Caspase-7 is activated during lovastatin-induced apoptosis of the prostate cancer cell line LNCaP," *Cancer Res.* **58**(1), 76–83 (1998).
  24. A. Periasamy and R. N. Day, "Visualizing protein interactions in living cells using digitized GFP imaging and FRET microscopy," *Methods Cell Biol.* **58**, 293–314 (1999).
  25. Y. Chen, M. Elangovan, and A. Periasamy, "FRET analysis: the Algorithm," in *Molecular Imaging: FRET Microscopy and Spectroscopy*, A. Periaswamy and R. N. Day, Eds., pp. 126–145, Academic Press (2005).
  26. S. F. Young, C. Griffante, and G. Aguilera, "Dimerization between vasopressin v1b and corticotropin releasing hormone type 1 receptors," *Cell Mol. Neurobiol.* **27**(4), 439–461 (2007).
  27. W. Guo, L. Shi, M. Filizola, H. Weinstein, and J. A. Javitch, "Crosstalkin G protein-coupled receptors: changes at the transmembrane homodimer interface determine activation," *Proc. Natl. Acad. Sci. U.S.A.* **102**(48), 17495–17500 (2005).
  28. M. Waldhoer, J. Fong, R. M. Jones, M. M. Lunzer, S. K. Sharma, E. Kostenis, P. S. Portoghese, and J. L. Whistler, "A heterodimer-selective agonist shows in vivo relevance of G protein-coupled receptor dimers," *Proc. Natl. Acad. Sci. U.S.A.* **102**(25), 9050–9055 (2005).